0888-8809/06/$15.00/0
Printed in U.S.A.

Molecular Endocrinology 20(9):2173–2186

doi: 10.1210/me.2005-0196

Diminished Growth and Enhanced Glucose Metabolism in Triple Knockout Mice Containing Mutations of Insulin-Like Growth Factor Binding Protein-3, -4, and -5

Yun Ning, Alwin G. P. Schuller, Sheri Bradshaw, Peter Rotwein, Thomas Ludwig, Jan Frystyk, and John E. Pintar

Department of Neuroscience and Cell Biology (Y.N., A.G.P.S., S.B., J.E.P.), University of Medicine and Dentistry of New Jersey, Piscataway, New Jersey 08854; Department of Biochemistry & Molecular Biology (P.R.), Oregon Health & Science University, Portland, Oregon 97201; Department of Pathology (T.L.), Columbia University, New York, New York 10032; and Institute of Experimental Clinical Research (J.F.), Aarhus University Hospital, Aarhus DK-8000, Denmark

IGF-I and IGF-II are essential regulators of mammalian growth, development and metabolism, whose actions are modified by six high-affinity IGF binding proteins (IGFBPs). New lines of knockout (KO) mice lacking either IGFBP-3, -4, or -5 had no apparent deficiencies in growth or metabolism beyond a modest growth impairment (~85–90% of wild type) when IGFBP-4 was eliminated. To continue to address the roles of these proteins in whole animal physiology, we generated combinational IGFBP KO mice. Mice homozygous for targeted defects in IGFBP-3, -4, and -5 remain viable and at birth were the same size as IGFBP-4 KO mice. Unlike IGFBP-4 KO mice, however, the triple KO mice became significantly smaller by adulthood (78% wild type) and had significant reductions in fat pad accumulation ($P < 0.05$), circulating levels of total IGF-I (45% of wild type; $P < 0.05$) and IGF-I bioactivity (37% of wild type; $P < 0.05$). Metabolically, triple KO mice showed normal insulin tolerance, but a 37% expansion ($P < 0.05$) of β-cell number and significantly increased insulin secretion after glucose challenge, which leads to enhanced glucose disposal. Finally, triple KO mice demonstrated a tissue-specific decline in activation of the Erk signaling pathway as well as weight of the quadriceps muscle. Taken together, these data provide direct evidence for combinatorial effects of IGFBP-3, -4, and -5 in both metabolism and at least some soft tissues and strongly suggest overlapping roles for IGFBP-3 and -5 in maintaining IGF-I-mediated postnatal growth in mice. (*Molecular Endocrinology* 20: 2173–2186, 2006)

IGF-I AND IGF-II ARE important determinants of mammalian growth, development, and metabolism (1–4). IGF bioactivity is modulated by a family of six IGF binding proteins (IGFBP-1 to -6), which are highly homologous proteins with high affinity for IGFs (3, 5, 6). The interaction of IGFBPs with IGFs generally blocks IGF receptor activation and inhibits IGF biological actions. These inhibitory effects of most, if not all, IGFBPs on IGF action have been reported in systems ranging from regulation of DNA synthesis, to blood glucose regulation and to body growth (7–9).

Under specific experimental conditions, however, various IGFBPs may instead potentiate the action of IGFs both *in vitro* and *in vivo*. For example, IGFBP-3 can enhance the IGF-I-mediated DNA synthesis in breast carcinoma cells (10) and osteoblasts (11) *in vitro* and also stimulate proliferation in PC-3 prostatic cancer cells by a process that depends on both active proteolysis of IGFBP-3 and the presence of IGF-I (12). *In vivo* studies have also shown that coadministration of IGF-I with IGFBP-3 was more effective in eliciting weight gain in hypophysectomized rats than an even larger dose of IGF-I alone (13). In addition, coadministration of IGF-I and IGFBP-3 can also accelerate wound healing (14), whereas injection of an IGF-I antibody that mimics the effect of IGFBP-3 *in vivo* led to increased muscle weight (16). In addition to these studies of IGFBP-3, other IGFBPs can also potentiate IGF action. For example, a single local injection of IGFBP-5 to the outer periosteum of the parietal bone of IGF-I KO mice increased ALP activity and osteocalcin levels of calvarial bone extracts (15). In addition to these specific effects, most IGFBPs also more generally act as carrier proteins in the bloodstream and are thought to regulate the efflux of IGFs from the vascular space (17–20). The IGF/IGFBP complexes pro-

First Published Online May 4, 2006

Abbreviations: ALS, Acid-labile subunit; ES, embryonic stem; H/E, hematoxylin and eosin; IGFBP, IGF binding protein; KO, knockout; KRB, Krebs Ringer buffer; TBS, Tris-buffered saline.

***Molecular Endocrinology* is published monthly by The Endocrine Society (http://www.endo-society.org), the foremost professional society serving the endocrine community.**

long the half-lives of IGFs and thus may buffer the potential hypoglycemic effects that could result from high concentrations of circulating unbound IGFs (21, 22).

The ability of IGFBPs to inhibit and stimulate effects IGF actions, or perhaps act independently, is a subject of ongoing interest, but the precise roles of individual IGFBPs *in vivo* are still largely unknown. This is due both to the complexity of IGFBP family number and regulation, as well as the fact that the majority of evidence has been derived from *in vitro* studies (7). Transgenic and knockout (KO) strategies in model organisms have provided unique opportunities to perform gain of function, partial loss of function, and loss of function studies for a particular gene. Several lines of transgenic mice overexpressing different IGFBPs generally show specific organ growth retardation (23), consistent with inhibitory effects on IGF action. Transgenic mice in which IGFBP-4 is overexpressed in smooth muscle, for example, exhibit a tissue-specific smooth muscle hypoplasia (24). In contrast to the transgenic studies, the single IGFBP KO mice reported to date have shown more modest phenotypes. For example, IGFBP-2 KO mice only show a reduction in spleen weight (25), whereas IGFBP-1 KO mice show normal size and metabolism but have deficits in liver regeneration (26). It is reasonable to speculate that functional compensation by other members of the IGFBP family may have prevented the appearance of more dramatic phenotypes in these lines. Thus, it is of interest to examine both the phenotype of additional IGFBP KO mice as well as the phenotype if multiple IGFBPs are deleted.

In this study, we generated individual IGFBP-3, -4, and -5 single null mice as well as IGFBP-3-4-5 triple null mice. We explored several aspects of the IGFBP-3-4-5 KO mouse phenotype, including growth rate, body composition, IGF-I and insulin levels, IGF-I bioactivity, ability to regulate glucose homeostasis, and the consequence on activation of the MAPK and AKT signaling pathways in muscle. Our study demonstrates overlapping crucial roles for IGFBPs in regulating development and metabolism *in vivo*.

RESULTS

IGFBP-3-4-5 Triple Null Mice Develop a Growth Deficit that Is Accompanied by Significant Decreases in Fat Pad Weight and Adipocyte Size

To determine whether the absence of a single IGFBP KO (IGFBP-3, -4, or -5) resulted in altered growth, offspring from heterozygous mating of each individual KO strain were weighed from birth to postnatal d 42. Body weights of both male and female IGFBP-3 and -5 single KO mice were indistinguishable from wild type during this period, demonstrating that pre- and postnatal growth was not affected by either the IGFBP-3 or IGFBP-5 mutations (Fig. 1, A and C). IGFBP-4 null mice were born with a 10–15% decrease in body weight and remained 10–15% smaller than wild-type mice in the postnatal period (Fig. 1B), demonstrating that only prenatal growth was impaired by the IGFBP-4 mutation. Although only the IGFBP-4 single KO mice show a modest growth deficit phenotype, IGFBP-3-4-5 triple KO mice exhibit a significantly greater growth retardation than IGFBP-4 mutant mice, which becomes significant at P20 ($\sim$78% of normal) and continues through at least 14 wk (Fig. 1D).

To further explore the body weight phenotype of IGFBP-3-4-5 KO mice, body length, major organ weight, and fat pad accumulation from both 9- and 14-wk-old mice were measured. Although there was a tendency toward a shorter snout-rump length, this did not reach significance, nor were there changes in weights of any major organs in mutant mice (Table 1 for 14-wk-old mice and, for 9-wk-old mice, Supplemental Table 1 published on The Endocrine Society's Journals Online web site at http://mend.endojournals.org). However, weights of all fat pads were significantly decreased in the mutant mice (Table 1 and Fig. 2A), which also showed a decreased weight of the quadriceps muscle (see below). To further explore the alteration in fat pad weight, the abdominal fat pads from both wild-type and mutant mice were histologically examined and the distribution of adipose cell area was determined. The mutant mice contain adipocytes that are much smaller compared with those from wild-type mice (Fig. 2B).

Serum IGFBPs, Blood Glucose, Total Circulating IGF-I Levels, and Bioactivity of IGF-I

Western ligand blotting of the sera from IGFBP-3-4-5 triple null mice, using ^{125}I-IGF-I as tracer, showed the disappearance of 38-kDa IGFBP-3 doublet and 24-kDa IGFBP-4 proteins (Fig. 3A), which were consistent with the genotype. However, an intermediate band that potentially reflects contributions from both IGFBP-1 and -2 in ligand binding studies was not significantly changed in mutant mice (Fig. 3A). We then directly compared the IGFBP-2 levels in wild-type and triple KO mice using Western blot. The triple KO mice also showed unchanged IGFBP-2 levels (Fig. 3A), which by inference indicated that there is also no significant change in IGFBP-1 levels.

After overnight fast, IGFBP-3-4-5 KO mice exhibited a significant reduction in blood glucose levels compared with wild-type mice (Fig. 3B). The total IGF-I levels in serum in mutant and wild-type mice were also determined after overnight fast via RIA, and it was found that IGFBP-3-4-5 triple KO mice had a more than 50% reduction in total serum IGF-I compared with wild-type mice (Fig. 3C). In addition to measuring total IGF-I in extracted serum, we also measured IGF-I bioactivity in those samples. This was achieved by determining the ability of serum to phosphorylate (*i.e.* to activate) the IGF-I receptor *in vitro* using cells transfected with the human IGF-I receptor. This assay was

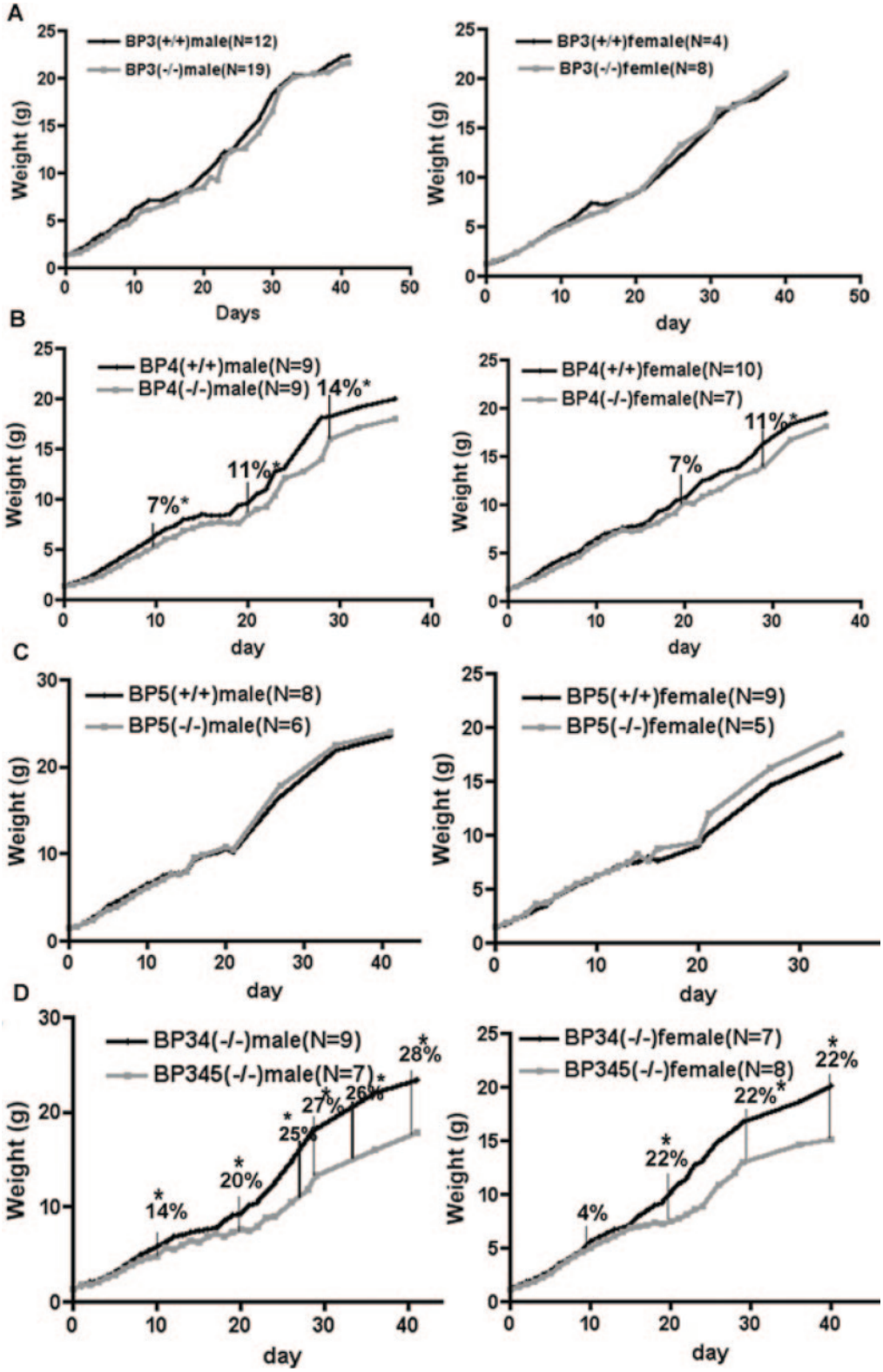

Fig. 1. Body Weights of IGFBP-3, -4, -5 Single KO Mice and IGFBP-3-4-5 Triple KO Mice

A, Male and female body weights of IGFBP-3 mice from heterozygous matings. B, Body weights of IGFBP-4 mice from heterozygous matings. Male and female body weights of IGFBP-4 null mice were 10–15% smaller than wild-type mice (*, $P < 0.05$). C, Male and female body weights of IGFBP-5 mice from heterozygous matings. D, IGFBP-3, -4, -5 mutant mice showed growth retardation beginning from the birthday (90% of normal), and this growth retardation becomes obvious after P20 (~80% of normal) and continues through the puberty (~72% for male mutant and ~22% for female mutant) compared with IGFBP-3, -4 mutant mice (*, $P < 0.05$).

Table 1. Body Composition and Fat Pad Composition in Wild-Type and IGFBP-3-4-5 Null Mice

Age 14 wk	Wild Type	% Body Weight	IGFBP345(−/−)	% Body Weight
Body weight	40.7 ± 2.1 g		32.5 ± 1.56 g	78.85[a]
Body length	96 ± 1.4 mm		93 ± 1.36 mm	
Heart	0.228 ± 0.02 g	0.56 ± 0.04	0.18 ± 0.01 g	0.56 ± 0.02
Liver	1.5 ± 0.06 g	3.68 ± 0.04	1.32 ± 0.018 g	4.06 ± 0.03
Kidney	0.54 ± 0.015 g	1.32 ± 0.06	0.44 ± 0.02 g	1.35 ± 0.05
Lung	0.2 ± 0.012 g	0.49 ± 0.03	0.2 ± 0.01 g	0.61 ± 0.05
Gonadal fat pad	2.24 ± 0.27 g	5.3 ± 0.39	0.67 ± 0.05 g	2.1 ± 0.16[a]
sc Fat pad	1.88 ± 0.25 g	4.5 ± 0.44	0.87 ± 0.07 g	2.6 ± 0.11
Perenal fat pad	0.95 ± 0.11 g	2.3 ± 0.18	0.35 ± 0.05 g	1.04 ± 0.14
Retroperitoneal fat pad	0.3 ± 0.04 g	0.7 ± 0.11	0.18 ± 0.03 g	0.5 ± 0.11
Total fat pad	5.5 ± 0.6 g	12 ± 0.1	2.13 ± 0.17 g	6.4 ± 0.4[a]

Data from 9-wk-old (see supplemental data for 9-wk-old mice) and 14-wk-old wild-type and IGFBP-3-4-5 KO mice (for each group in each genotype, $n > 6$) are presented. The whole body weight, body length, different organ weights, and fat pad weight from gonadal, sc, perenal, and retroperitoneal fat pad were measured. Because the IGFBP-3-4-5 KO mice exhibit 23% reduction in body weight compared with wild-type mice, the organ weights and fat pad weights were calculated as percentage of the whole body weight and then compared via Student's *t* test. Although there is a tendency toward decreased snout-rump length, there is no significant difference in body length and different organ weights in both 9- and 14-wk-old wild-type and mutant mice. However, there is a significant decrease in fat pad weights in mutant mice compared with wild-type mice in both ages ([a], $P < 0.05$).

first presented in Ref. 27 and is also described in detail *in Materials and Methods*. This cell-based bioassay showed that IGF-I bioactivity was even more markedly suppressed in IGFBP-3-4-5 KO mice (37% of wild-type levels) as compared with total IGF-I (Fig. 3D). Overall, the IGF-I levels were clearly decreased in mutant mice and we suggest that, following loss of IGFBP-3, IGFBP-5 and IGFBP-4, the mutant mice cannot efficiently stabilize IGF-I in circulation. As a consequence, the triple KO mice exhibit a significant decrease in IGF-I bioactivity, which leads to the enhanced growth deficit in those mice.

Enhanced Glucose Homeostasis in IGFBP-3-4-5 Null Mice

Because IGFBPs regulate the bioavailability of IGF-I that, like insulin, can mediate glucose uptake and metabolism (22), we tested whether the deletion of individual or combined IGFBPs may affect glucose disposal by investigating glucose tolerance in mutant mice after an overnight fast. The responses to a glucose challenge were decreased in IGFBP-4 mutant mice at 60 min and 90 min, whereas IGFBP-3 and -5 mutant mice showed a normal glucose responses compared with wild-type mice (see supplemental Fig. 2). However, glucose levels after glucose challenge were significantly decreased in BP-3-4-5 triple KO mice compared with wild-type mice as well as IGFBP-3 and IGFBP-5 KO mice over a broad time range (from 30–120 min after glucose injection). Moreover, the decrease of glucose in triple mutant mice was significantly enhanced compared with IGFBP-4 mutant mice (Fig. 4A). This result indicated that the mutant mice have increased glucose uptake that is probably due to the combined effect of deletion of three IGFBPs.

To further explore mechanisms underlying the enhanced glucose homeostasis in triple KO mice, we measured insulin and IGF-I levels in IGFBP-3-4-5 null mice after glucose challenge. During the first hour after glucose injection, the secretion of insulin typically exhibits two phases: the first phase consists of a rapid secretion of insulin that lasts from 0–10 min and leads to the highest insulin peak; the second phase is characterized by the reduced insulin secretion and lasts from 10–60 min (28). Although insulin levels in both IGFBP-3-4-5 KO mice and wild-type mice increased after glucose injection, IGFBP-3-4-5 triple KO mice exhibited significantly higher insulin levels compared with wild-type mice not only during the first phase at 1 and 2 min but also higher insulin levels during the second phase of insulin secretion at 15 and 30 min (Fig. 4B). Therefore, increased insulin secretion after glucose challenge appears to contribute to the enhanced glucose clearance in triple KO mice. This finding was also consistent with the increased islet area observed in triple KO mice (see below).

IGF-I levels were also examined following glucose challenge. The IGF-I levels in wild-type mice showed a slight increase after glucose challenge. The IGF-I levels in IGFBP-3-4-5 triple KO mice reached a peak at 30 min and then dropped back to normal levels by 60 min. It is notable that IGFBP-3-4-5 triple KO mice exhibited lower circulating IGF-I levels compared with wild type at all time points examined in this experiment, similar to the lower levels seen after overnight fast (Fig. 4C). However, when the percentage of increase in IGF-I levels between these strains was compared, it was found that IGFBP-3-4-5 triple KO mice had an significantly larger percentage of increase in total IGF-I compared with wild-type mice at 30 min (43%), whereas the wild-type mice only exhibited a slight percentage of increase in total IGF-I at 30 and 60 min (6% and 8%, respectively) (Fig. 4D). Therefore, this transient increase in circulating IGF-I might also contribute to the enhanced glucose homeostasis, al-

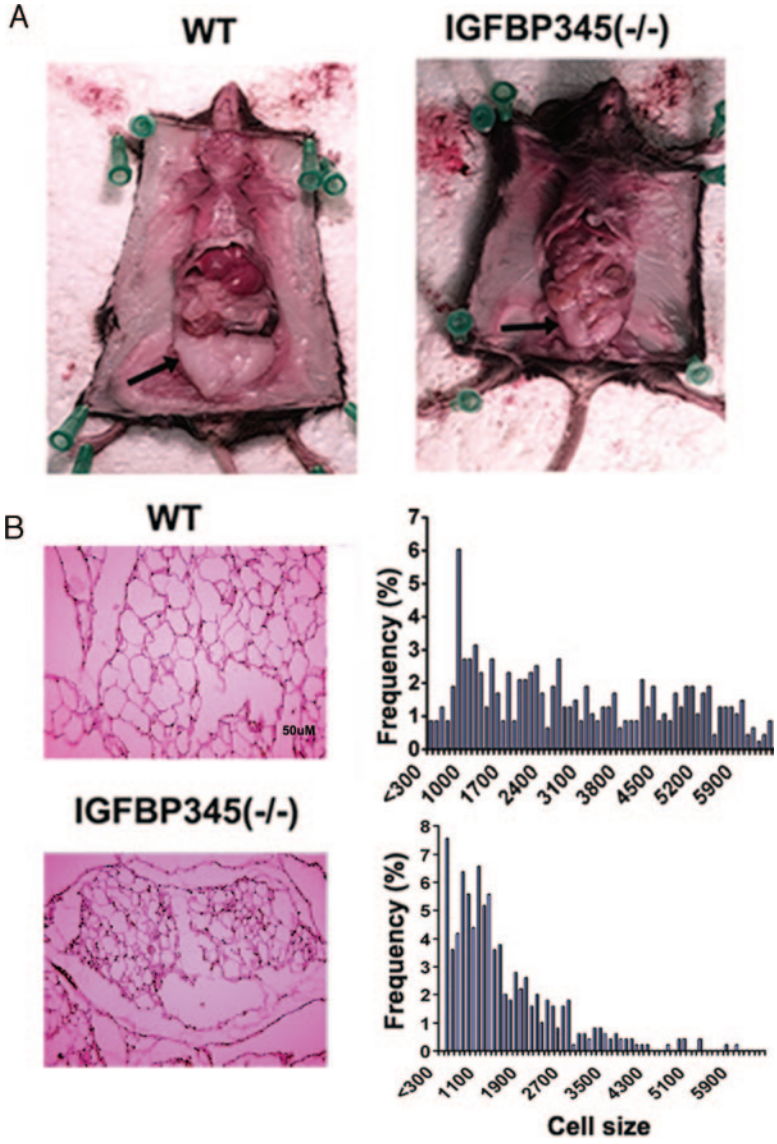

Fig. 2. Fat Pad Accumulation Is Significant Decreased in IGFBP-3-4-5 Triple KO Mice

A, The fat pads in IGFBP345(−/−) mice were significantly smaller than that in wild-type mice (photo representative from n >5 in each genotype; also see Table 1). B, Histology of the abdominal fat pad from both wild-type and IGFBP345(−/−) mice (stained with H/E) at age 9 wk is shown at *left*. *Bar*, 50 μm. The distribution of adipocyte size in wild-type and triple KO mice is shown at right. The size (μm^2) of at least 300 cells per sample from five different mice per group was determined using Image J software (NIH).

though more studies need to be done to determine whether this increase is reflected by increased free or bioactive IGF-I.

Islet Area Is Increased, whereas Insulin Sensitivity Is Unchanged in IGFBP-3-4-5 Null Mice

Because IGFBP-3-4-5 null mice showed a significantly enhanced glucose uptake and at the same time had higher circulating insulin levels following glucose challenge as compared with wild-type animals, it was valuable to measure insulin sensitivity using the insulin tolerance test. The result revealed that the adult triple KO mice exhibited normal insulin sensitivity compared with wild-type mice (Fig. 5A).

IGFs and insulin are important in regulating β-cell differentiation, proliferation, and survival via insulin/IGF-I signaling pathways (29). Deletion of insulin receptor substrate-1 produces small, insulin-resistant mice with nearly normal glucose homeostasis due to compensatory β-cell expansion (30). In contrast, mice lacking insulin receptor substrate-2 display nearly normal growth, but develop diabetes 8–10 wk after birth accompanied by reduced β-cell mass and impaired function (31). Therefore, the lower circulating IGF-I level and higher insulin secretion in triple KO mice after glucose challenge prompted us to analyze islet morphology of the mutant mice. In adult IGFBP-3-4-5 null mice, hematoxylin and eosin (H/E) staining of pancreatic sections revealed that

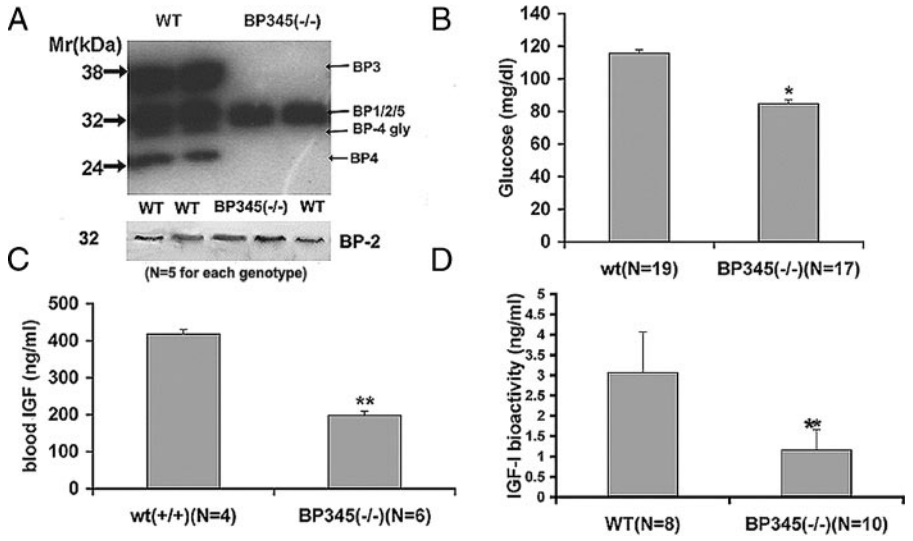

Fig. 3. Serum IGFBPs, Blood Glucose, Total Circulating IGF-I Levels and Bioactivity of IGF-I in Wild-Type and IGFBP-3-4-5 Triple KO Mice

A, IGFBP expression in wild-type (WT) and IGFBP-3, -4, -5 triple KO mice. Serum from WT and triple KO mice (n = 5 for each genotype) was assayed by Western ligand binding experiment (*upper panel*) and immunoblot (*lower panel*). Loss of 24-kDa IGFBP-4 and 38- kDa IGFBP-3 bands confirmed the mouse genotype. There is no dramatic change in intermediate band (32 kDa) that contained the contribution from both IGFBP-1 and -2. Moreover, there is no significant change in IGFBP-2 band from Western blot in mutant mice. B, Serum glucose levels following overnight fasting in WT and IGFBP-3-4-5 mutant mice. Mutant mice (84 $\pm$ 2.8 mg/dl) have a significant decrease in circulating glucose compared with wild-type mice (115 $\pm$ 3 mg/dl) (*, $P < 0.05$). C, Total circulating IGF level in IGFBP-3-4-5 null mice is decreased compared with wild-type mice. IGFBP345 triple KO mice (198 $\pm$ 11 ng/ml) have significantly lower levels (47%) of total IGF-I in serum compared with wild-type mice (418 $\pm$ 21 ng/ml) (**, $P < 0.01$). D, Bioactivity of IGF-I is significantly decreased in fasted IGFBP-3-4-5 KO mice. Bioactivity level of IGF-I in IGFBP345 triple KO mice (1.16 $\pm$ 0.5 ng/ml) is significantly decreased (**, $P < 0.01$) compared with the level in wild-type mice (3.12 $\pm$ 1 ng/ml), which is consistent with the significant decrease in circulating IGF-I in triple KO mice. The decreased bioactivity of IGF-I may result from both decreased IGF-I level or/and deletion of IGFBPs. These data are consistent with the possibility that the growth deficit in IGFBP-3-4-5 KO mice results from the decrease in bioactive IGF-I.

morphology of islets appeared normal in both wild-type and triple KO mice (Fig. 5B). However, β-cell area in adult IGFBP-3-4-5 null mice was significantly increased about 37% (Fig. 5, C and D). These findings were consistent with the increased insulin secretion seen in the glucose tolerance experiment described above. Therefore deletion of IGFBPs leads to an increased β-cell area that accompanies the enhanced insulin response to glucose challenge.

Erk Signaling Pathway and Weight of Quadriceps Muscle Are Significantly Decreased in IGFBP-3-4-5 Null Mice

Insulin and IGF-I bind to distinct cell-surface receptor tyrosine kinases that regulate a variety of signaling pathways controlling metabolism, growth, and survival (32–34). IGFBP-3-4-5 null mice had lower circulating IGF-I levels but higher insulin levels and proportionally increased IGF-I levels after glucose challenge. All of these changes indicate that IGFBP-deficient mice might also have alterations in downstream signaling pathways. We investigated Erk/MAPK and AKT phosphorylation in muscle of triple KO mice because muscle is the one of the major sites for the mitogenic and metabolic effects of IGF-I and insulin (35). IGFBP-3-4-5 triple KO mice showed a slightly increased AKT activation level and a significantly decreased Erk/MAPK activation level (72%) compared with wild type (Fig. 6, A and B). Moreover, the quadriceps femoris skeletal muscle from the triple KO mice was smaller than that of wild type (Fig. 6C), which is consistent with the decreased Erk/MAPK activation, and thus appears to contribute, along with the lower fat pad accumulation (see above), to the lower body weight of the triple KO mice.

DISCUSSION

Growth Retardation in IGFBP-3-4-5-Deficient Mice

Although both IGF ligands are required for normal pre- and postnatal growth, the roles of IGFBPs in these processes have been uncertain. We here report that both IGFBP-3 and -5 single KO mice exhibit normal growth, whereas IGFBP-4 KO mice exhibit a prenatal growth deficit. Because IGFBP-3 and IGFBP-5 are the only IGFBPs known to contribute to formation of the ternary IGF-IGFBP-acid-labile subunit (ALS) complex that normally stabilizes the IGFs (19), the normal growth in those two single KO mice, compared with

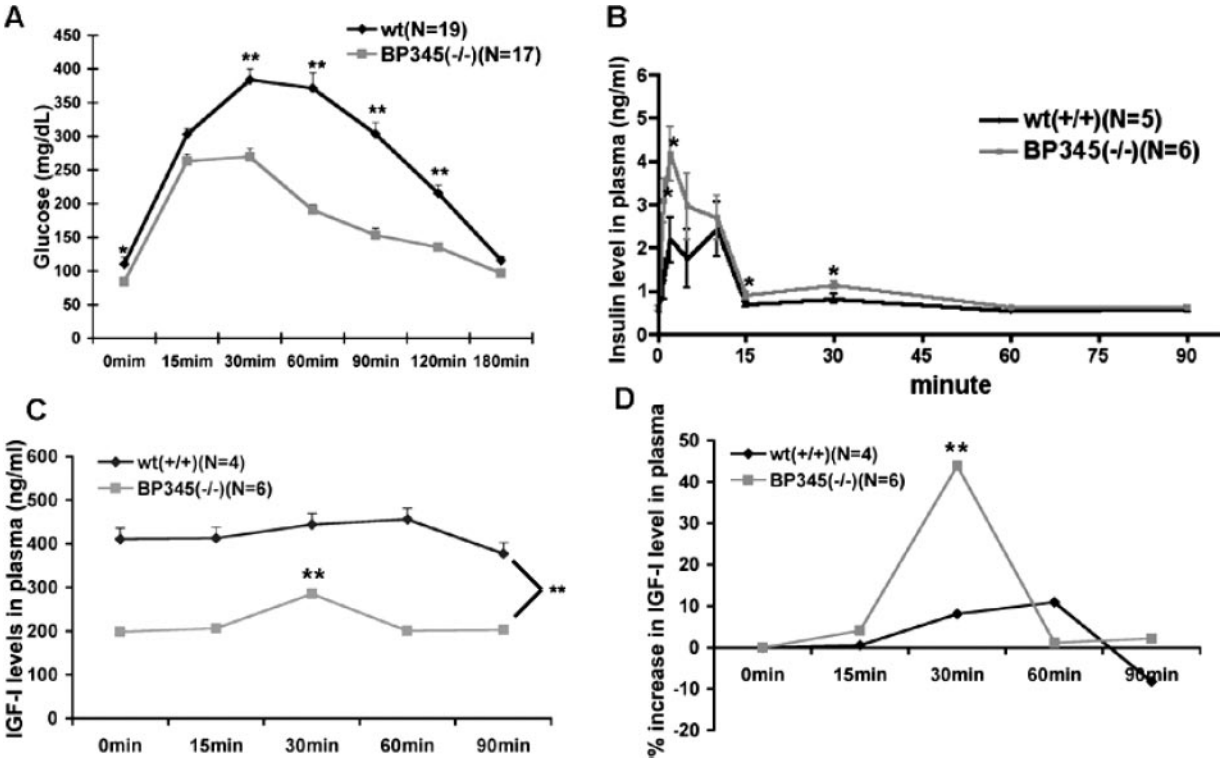

Fig. 4. Enhanced Glucose Homeostasis in IGFBP-3-4-5 Null Mice

A, Increased glucose tolerance in IGFBP-3-4-5 KO mice: mice were administrated 2 g/kg body weight D-glucose (ip) after overnight fast. Glucose levels were monitored in tail blood at 0, 15, 30, 60, 90, 120, and 180 min. The responses to a glucose challenge after overnight fasting were significantly enhanced in IGFBP-3-4-5 KO mice ($P < 0.01$ at 0, 30, 60, 90, and 120 min compared with wild-type mice). B, Increased insulin secretion after glucose injection in IGFBP-3-4-5 mutant mice: after glucose injection, insulin levels in both IGFBP-3-4-5 KO mice and wild-type mice were increased. However, insulin levels of IGFBP-3-4-5 KO mice were significantly higher than wild type (WT) at 1 and 2 min during the first phase (*, $P < 0.05$) and at 15′ and 30′ during the second phase (*, $P < 0.05$). C, Lower circulating IGF-I levels in IGFBP-3-4-5 mutant mice in glucose tolerance experiment: The IGF-I levels in IGFBP-3-4-5 triple KO mice reached the highest peak around 30 min (285 ± 23ng/ml), whereas the IGF-I level in wild type reached the highest peak at 30 min and last to 60 min (444 ± 45 ng/ml; 455 ± 37 ng/ml). In all, IGFBP-3-4-5 KO mice had significant lower amount of total IGF-I (**, $P < 0.01$) at all listed time points (0–90 min). D, Triple KO mice have lower IGF-I levels but larger percentage of increase in IGF-I secretion after glucose injection: IGF-I levels in IGFBP-3-4-5 triple KO mice were increased by 43% at 30 min, whereas IGF-I levels in wild-type mice were increased by 6%, 8% at 30 and 60 min, respectively. Thus, although IGFBP-3-4-5 KO mice had significantly lower amount of total IGF-I (*, $P < 0.05$) under the normal circumstances, after glucose injection, IGFBP-3-4-5 KO mice had larger increase in IGF at 15 and 30 min, indicating a transient increase in the total IGF-I in the mutant mice.

mice lacking both these genes (see below), likely results from the abilities of either IGFBP-3 or -5 to stabilize sufficient levels of IGF needed for normal growth. Additional work to examine the binding characteristics of labeled IGF-I with serum proteins from these different genotypes will be needed to directly determine whether this in fact occurs.

IGFBP-4 single KO mice exhibit a 10–15% modest growth deficit at birth, which demonstrates that IGFBP-4 is required for normal prenatal growth. Importantly, other IGFBPs cannot compensate fully, if at all, for IGFBP-4 absence. When compared with three single KO mice, the IGFBP-3-4-5 deficient mice also exhibited a modest growth retardation at the day of birth, similar to the growth deficit exhibited by IGFBP-4 KO alone. In contrast to the single IGFBP-4 KO, however, the growth deficit became significantly more extensive after P20 and was accompanied by significantly decreased fat accumulation and quadriceps muscle mass, and a significant reduction in circulating levels of IGF-I immunoactivity and bioactivity. Previous work has shown that lack of IGF-I results in both an intrauterine growth retardation and a postweaning growth deficit (36). Because both IGFBP-3 and -5, which are the only IGFBPs known to combine with ALS and IGF-I to form a ternary complex, are both deleted in the triple KO mice, one possibility that is consistent with the data is that the ability to form the ternary complexes is greatly reduced in these mutant mice, which is reflected by the lower circulating IGF-I levels. This hypothesis is also consistent with the observation that ALS-KO mice have markedly reduced IGF-I and IGFBP-3 levels and exhibit a modest reduction in postnatal growth (37). Moreover, the lower cir-

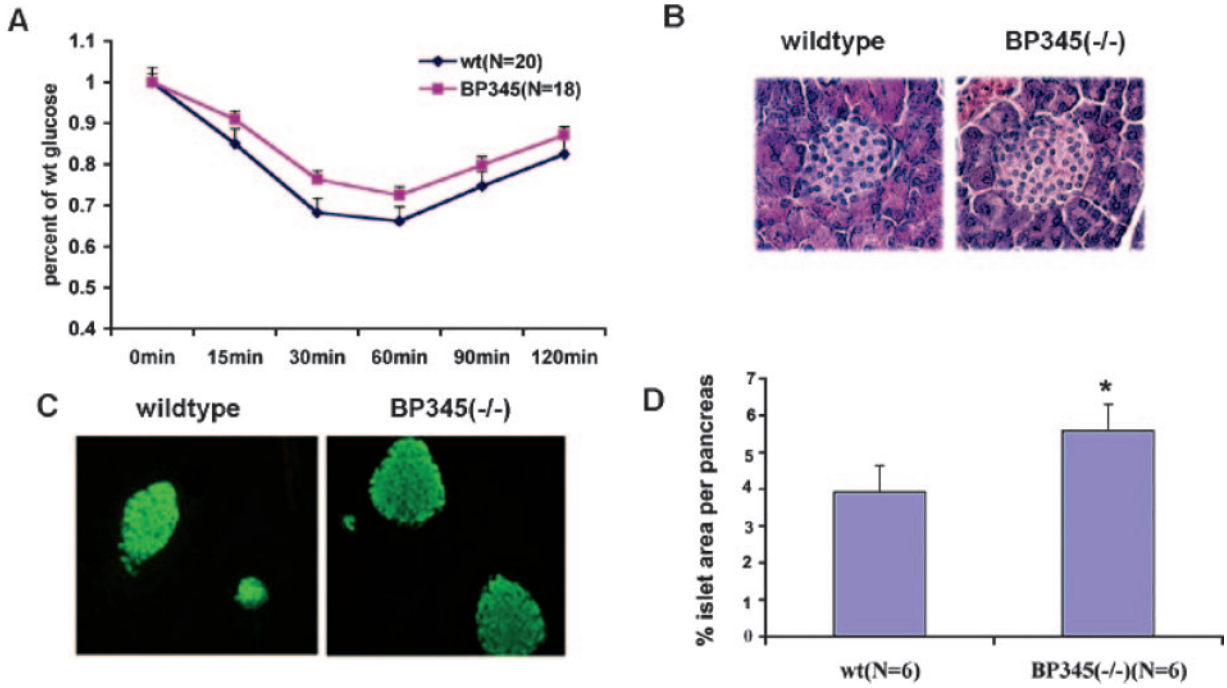

Fig. 5. Insulin Sensitivity Is Not Significantly Changed, whereas Islet Mass Is Significantly Increased in IGFBP-3, -4, -5 Mutant Mice

A, There is no significant change in insulin sensitivity in mutant mice: Insulin (ip 0.5U/kg) is injected into overnight fasted adult BP-3-4-5 KO and wild-type mice. Blood from the tail vein of two types of mice were assayed using glucose meter. There was no significant change ($P > 0.05$) in glucose level in triple KO mice, indicating that insulin sensitivity is not altered in KO mice. B, H/E staining of islets: H/E staining shows normal morphology of islets in KO mice. C and D, Fluorescent isothiocyanate staining of β-cell area: for analysis of adult pancreata, pancreas were embedded in paraffin and consecutive sections (15 μm) were collected and mounted. Then one out of four continuous slides were immunostained using mouse antiinsulin antibody, followed by detection using fluorescent antibodies to visualize the β-cell. For quantitation of β-cell area, the entire stained areas were viewed using fluorescent microscope and digitally photographed at a magnification of $\times$100. The entire sections were digitally photographed at a magnification of $\times$2, and analyses of β-cell area and entire section areas were performed using Matlab software. Average percentage of islet area per pancreas was calculated from the total count of 24 sections out of 96 sections from each mouse (totally over 600 islets in all cross sections). From a total of six wild-type mice and six IGFBP-3-4-5 mutant mice, fluorescent isothiocyanate staining islet area was significantly increased (37%) (*, $P < 0.05$) in KO mice, consistent with the higher insulin secretion in glucose challenge.

culating IGF-I levels in the triple KO mice are accompanied by a even greater decrease in IGF-I bioactivity (~1/3 of wild-type level), which would be sufficient to lead to the pronounced post-weaning growth deficit observed in these mice. Although liver-specific IGF-I null mice exhibit a 75% decrease in circulating IGF-I levels, these mice, unlike the triple KO mice, continue to exhibit normal levels of free IGF-I (38) and thus normal growth and development (39). Our finding suggests that IGF-I needs to be stabilized by the binding proteins to retain sufficient bioactivity to provide effective growth stimulation. However, we cannot exclude the possibility that the decreased bioactivity of IGF-I in serum from the triple KO mice may result from the combined effects of both decreased IGF-I and deletion of IGFBPs. In addition, it is possible that IGF-I-independent growth effects of the deleted IGFBPs and/or local growth effects of the remaining IGFs contribute to the overall size and tissue development in triple KO mice.

IGF-I serves as a growth-essential peptide by binding to the distinct cell-surface receptor tyrosine kinases that control growth and development (32–34, 40). One of the most important signaling pathways activated by IGF-I is the MAPK pathway. Tyrosine phosphorylation and activation of MAPK can serve as signal for cell growth, differentiation, and survival (41, 42). In our study, the triple KO mice showed significantly decreased activation levels of MAPK (72% of wild-type levels) in muscle. Moreover, the weight of quadriceps femoris skeletal muscle from IGFBP-3-4-5 KO mice was significantly smaller than that of wild-type mice. Together, those findings indicate that overall muscle weight may also be reduced and contribute to the body weight reduction in mutant mice. This possibility is supported by other *in vivo* models. For example, enhancement of muscle mass is seen in transgenic mice expressing IGF-I locally in the skeletal muscle (43), whereas IGF-I KO mice display features of severe muscle loss (44). However, more studies are

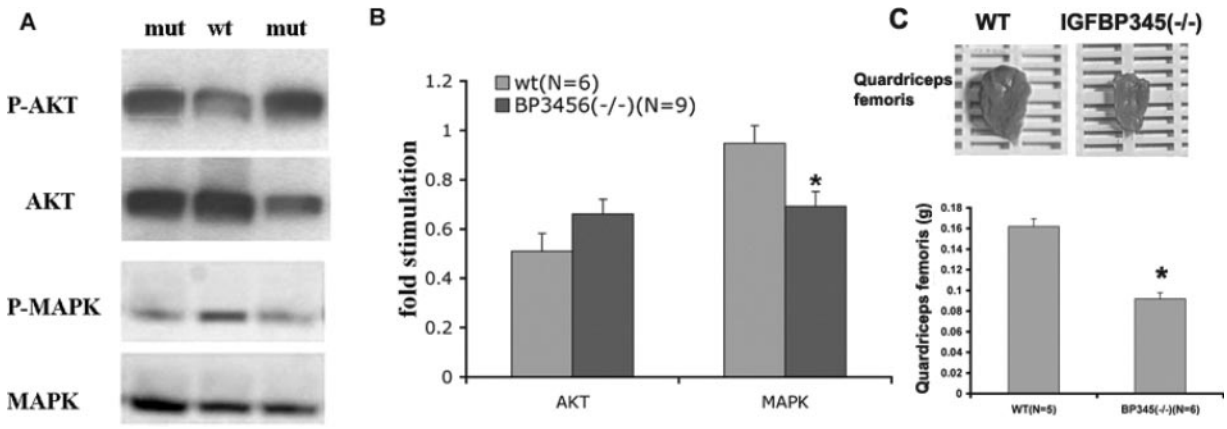

Fig. 6. MAPK and AKT Signaling Pathways in Muscle of IGFBP-3-4-5 KO Mice and Wild-Type Mice

A, Western blot analysis of phosphorylation of AKT and MAPK in muscle after overnight fast in IGFBP-3-4-5 KO mice and wt (wild type) mice. Levels of phosphorylation signals (P) are normalized to total immunoreactivity of AKT and MAPK. B, There is a slight increase in AKT activation and a significant decrease (*, $P < 0.05$) in MAPK activation. C, The quadriceps femoris skeletal muscle of IGFBP-3-4-5 KO mice is significantly smaller than that of wild-type mice ($n > 5$ in each genotype) (*, $P < 0.05$).

needed to explore the locations and onset of decreased muscle mass in the mutant mice.

The major change in tissue organization noted so far in the triple IGFBP KO mice is that the weights of all peripheral fat pads are significantly reduced and that the adipocytes are smaller in size compared with wild-type mice. Recent *in vivo* studies have demonstrated a role for IGF-I in adipocyte formation. Transgenic mice overexpressing leptin, which is characterized by a reduced plasma levels of glucose and IGF-I, exhibit a 75% decrease in adipocyte size (45), Therefore, the two thirds decrease in circulating bioactive IGF-I present in IGFBP-3-4-5 KO mice may thus be a critical factor that leads to the significant decrease in adipocyte size and thus total fat accumulation in these mice at the ages analyzed.

Metabolic Abnormalities in IGFBP-3-4-5-Deficient Mice

Initial metabolic analysis indicated that IGFBP-3-4-5 null mice exhibited lower fasting glucose levels, significantly decreased circulating IGF-I levels, significantly decreased IGF-I bioactivity and significantly increased insulin secretion after the glucose challenge. Thus, one goal of this study became to investigate whether IGFBP loss affects glucose metabolism by regulating insulin, regulating the bioavailability of IGF-I, or both.

Insulin has multiple reciprocal interactions with IGF-I and its binding proteins. For example, *in vivo* studies of IGF-I administration have consistently shown an inhibitory effect on insulin secretion (46). In muscle-specific insulin receptor KO mice, IGF-I levels increase to compensate for the lowered glucose uptake resulting from the lack of insulin signaling (47). Thus, the increased insulin level might be a response to the lower circulating IGF-I level in triple KO mice. In addition to these effects, it has been reported that IGF-I at physiological concentrations can inhibit insulin secretion *in vivo* (48), so the decreased IGF-I level in triple KO mice may release this inhibition on insulin secretion, thereby explaining the increased insulin secretion. The morphological analysis of the pancreas in triple KO mice showed a significant increase in the islet area, which likely contributes to the compensatory increase in insulin secretion following the glucose challenge. Increased insulin activation of its cell-surface receptor would result in increased activation of phosphatidylinositol-3 kinase and subsequent formation of phosphatidylinositol-3 phosphate, which could serve to increase glucose transport (49, 50). The triple KO mice also showed slightly increased activation levels of AKT in muscle, which is consistent with the increased insulin secretion.

IGF-I has been reported to have potent antiapoptotic activity in islet cells. Exogenous IGF-I blocks the *in vitro* cytokine-induced apoptosis of these cells (51) and human islets transfected with the IGF-I gene are also resistant to IL-1β-induced and Fas-mediated apoptosis (52). Our study shows that mutant mice have a significant increase in islet cell area in the pancreas, which suggests that the lower circulating IGF-I level in mutant mice are not sufficient to enhance apoptosis of islet cells.

Whereas insulin is the key short term regulator of glucose homeostasis, emerging evidence suggests that the IGF-I contributes to long-term glucose homeostasis (22, 53, 54). The insulin-like activity of IGF-I has been estimated to be 5–10% that of insulin (55). Based on the high circulating IGF-I concentration, the insulin-like potential of IGF-I far exceeds that of insulin itself (IGF-I: 100- 800 ng/ml *vs.* insulin: 1–4 ng/ml) and yet does not cause hypoglycemia, apparently because it is sequestered into 150-kDa complexes with either IGFBP-3 or IGFBP-5 and ALS. In our study, although

IGFBP-3-4-5 KO mice consistently exhibited a significantly lower circulating IGF-I after glucose challenge, the mutant mice showed a transient large percentage of increase in IGF-I compared with their lowered baseline. Thus, the increase of total IGF-I in the circulation, combined with the depletion of IGFBPs that would sequester IGF-I, could be expected to lead to a transient increase in bioactive IGF-I. This hypothesis is consistent with a previous study in which administration IGFBP-3 to the mouse temporarily depleted free IGF and caused a rise in plasma glucose (3). A similar observation was made when IGFBP-1 was administered as an iv bolus in the rat (56), where plasma glucose levels increased transiently by approximately 10%. Thus, we postulate that deletion of IGFBPs attenuates the ability of IGFBPs to buffer IGF bioavailability. As a consequence, there is a comparatively larger transient increase in bioactive IGF-I when the mice are given a glucose challenge, which, along with insulin, may also contribute to the enhanced glucose homeostasis. However, direct bioactive IGF-I measurement in the glucose challenge is needed to test this hypothesis.

Taken together, we have demonstrated that the significant decrease in circulating IGF-I in mutant mice is accompanied by a significant increase in insulin secretion and islet expansion. As a consequence, the mutant mice exhibit an enhanced glucose clearance. Moreover, because mutant mice also showed a transient increase in IGF-I levels after glucose challenge, altered tissue availability of circulating IGF-I may also contribute to the enhanced glucose homeostasis.

Conclusion

This study indicates that individual absence of IGFBP-3 and -5 do not affect growth, indicating possible compensation by the remaining IGFBPs, whereas the absence of IGFBP-4 cannot be fully compensated prenatally by other IGFBP family members. However, when the two major IGFBPs (IGFBP-3 and IGFBP-5) known to contribute to the ternary IGFBP-ALS-IGF complex are deleted, together with IGFBP4, the remaining IGFBPs appear to unable to prevent development of significant growth and metabolic disruptions. Deletion of these multiple IGFBPs then results in a significant post-weaning decrease in body weight that is more severe than modest growth deficit of the IGFBP-4 KO mice and appears to result from a significant decrease in bioactive IGF-I. The triple KO mice also exhibit impaired fat pad accumulation that is accompanied by a decrease in adipocyte size. Moreover, the triple KO mice exhibit decreased muscle weight that may result from decreased Erk activation. In addition, the deletion of multiple IGFBPs also leads to an increased response to glucose challenge, which appears to result primarily from the significant increase in insulin secretion that reflects islet expansion. Taken together, these genetic findings indicate that IGFBPs have critical but complex roles in growth and metabolism in the mouse.

MATERIALS AND METHODS

Production and Characterization of IGFBP-3-Deficient Mice

Screening of a 129ReJ genomic library with a digoxigenin-labeled rat IGFBP-3 cDNA resulted in the identification and isolation of three overlapping phage clones containing parts of the mouse IGFBP-3 gene. One of these clones was analyzed in more detail using restriction mapping and sequencing and served as a template to create the targeting construct. A 3.6-kb *Sac*II/*Kpn*1 fragment containing part of exon1 up to part of exon3 was cloned between neo and HSV-TK gene of the KO vector. Another 8.5-kb *Xho*1 fragment including 5′ of the translation start site of IGFBP-3 gene was cloned into the KO vector. Introduction of this targeting construct into CCE embryonic stem (ES) cells resulted in 142 G418 and gancyclovir-resistant ES clones. Genomic southern screening of DNA isolated from 142 individual ES clones identified 10 targeted line in which part of exon1, including the translation start site of IGFBP-3 and the signal peptide, was replaced by the neomycin resistance cassette. ES cells from this targeted line were injected into C57BL/6J blastocysts and transferred into pseudopregnant females to generate germline transmitting chimeras. Male chimeras were bred with C57BL/6J females to obtain mice carrying the IGFBP-3 mutant allele (see supplemental Fig. 1).

Production and Characterization of IGFBP-4-Deficient Mice

To generate IGFBP-4 KO mice, a 5-kb *Hin*dIII/*Bst*I fragment containing part of intron1 was cloned between neo and HSV-TK gene of the KO vector. Another 2.5-kb *Bst*X1/*Nru*I fragment was cloned into the KO vector (see supplemental data). The rest of procedures are the same as the procedure described above.

Production and Characterization of IGFBP-5-Deficient Mice

To generate the IGFBP-5 KO mice, a 9-kb *Eco*RI/*Sal*I fragment containing part of intron1 up to part of exon4 was cloned between neo and HSV-TK gene of the KO vector. Another 1.3-kb *Pvu*II/*Eco*RV fragment was cloned into the KO vector (see supplemental data). The rest of procedures are the same as the procedure described above.

Southern Analysis Genotyping

Mouse tail tip DNA was digested with *Sac*I (for IGFBP-3 genotyping), *Bam*HI (for IGFBP-4 genotyping), and *Eco*RI (for IGFBP-5 genotyping), respectively, run on 0.7% agarose gels and transferred to Hybond (Amersham). Membranes were prehybridized for 1 h at 65 C in Rapid Hyb (Amersham) and then hybridized overnight at 65 C in the same solution containing ^{32}P-labeled probe derived from fragment, shown in Fig. 1. Membranes were washed at 68 C in 1× saline sodium citrate/0.1% sodium dodecyl sulfate three times for 1.5 h, and then exposed to film. For IGFBP-3 genotyping, both a wild-type 6.9-kb fragment and a mutant 6-kb fragment were observed in *Sac*I-digested DNA from IGFBP-3 heterozygous mice. For IGFBP-4 genotyping, both a wild-type 9-kb fragment and a mutant 5.5-kb fragment were observed in *Bam*HI-

digested DNA from IGFBP-4 heterozygous mice. For IGFBP-5 genotyping, both a wild-type 4-kb fragment and a mutant 2-kb fragment were observed in *Eco*RI-digested DNA from IGFBP-5 heterozygous mice (see supplemental Fig. 1).

RT-PCR Analyses

Total RNA was purified from key tissues (kidney, brain, heart, and liver) (n = 3 per genotype) by using the RNeasy Midi protocol (QIAGEN, Valencia, CA) and analyzed by RT-PCR. The primers were chosen based the sequence of exon1 from IGFBP-5 gene. The 5′ primer sequence is GCTCGCCG-TAGCTCTTTTC and 3′ primer sequence is GGTTCTTTCGT-GCACTGTGA. The expected amplified fragment is 261 bp.

Generation of IGFBP-3-4-5 Null Mice by Cross-Breeding

IGFBP-3 null mice on a mixed 129/C57 background were first cross-bred with IGFBP-4 null mice. The double heterozygous mutants were intercrossed to generate IGFBP-3-4 null mice that were no different in size than IGFBP-4 mutant mice (data not shown). The homozygous IGFBP-3-4 null mice were then cross-bred with IGFBP-5 null mice. After the triple heterozygous were crossed for two generations, IGFBP-3(−/−)4(−/−)5(+/−), IGFBP-3-4-5 null mice and genetically similar littermate wild-type mice were obtained. IGFBP-3(−/−)4(−/−)5(+/−) mice were mated to establish the comparison between triple mutant and IGFBP-3-4 double mutant growth curve. The wild-type mice and the IGFBP-3-4-5 null mice arising from this cross-breeding continued to be intercrossed to produce the wild-type control and triple KO mice used in subsequent experiments. All mice used in the subsequent experiments were 2–4 months old and on a C57Bl6/129S6 mixed background.

Measurement of Postnatal Growth, Organ Size, Fat Pad, and Skeletal Muscle

IGFBP-3-4-5 null mice and IGFBP-3-4 null mice were first obtained from the IGFBP3(−/−)4(−/−)5(+/-) mating to examine any effects resulting from combined IGFBP-3 and IGFBP-5 deficiency on IGFBP-4 null background. Litters from IGFBP-3(−/−)4(−/−)5(+/-) mating were then analyzed from postnatal d 0 (day of birth) until 30 d, and then once per week for 2 months. Postnatal litters were ear marked, tail clipped for genotyping and weights of individuals were correlated with genotypes from the southern blotting of tail DNA. The adult mice were dissected and different organs (heart, liver, kidney, and lung) were collected and measured. Fat pad are mainly accumulated in four sites: sc, gonadal, perirenal, and retroperitoneal. Adult mice were dissected and fat pads from those four sites were collected and measured. Results are presented as fat content in percentage of total body weight. The freshly isolated gonadal white adipose tissues were fixed overnight in 10% formalin, dehydrated, embedded in paraffin and stained with H/E. The cell size was analyzed using ImageJ software (National Institutes of Health, Bethesda, MD). At least 300 cells from each animal were measured. The quadriceps femoris skeletal muscle was separated and weighed from both wild-type and mutant mice.

Western Ligand Blotting and Western Blotting

One to 3 μl serum from each animal was run on 12–16% polyacrylamide gels using either the Mini-Protean II or the Protean IIxi system (Bio-Rad Laboratories, Inc., Richmond, CA). Samples were electrophoresed and run through 5- to 6-cm gels at 85 V for approximately 3 h. Proteins were transferred to a polyvinylidene fluoride nylon membrane (Millipore Corp., Bedford, MA) which provided a signal intensity equivalent to that observed after transfer to nitrocellulose. Membranes were preblocked with 1% BSA in Tris-buffered saline (TBS) containing 3% Nonidet P-40 and 0.1% Tween 20 before overnight incubation with 400,000 cpm of ^{125}I-IGF-I at 4 C (to show the remaining IGFBPs) or incubation with IGFBP-2 Ab (Upstate Corp., Lake Placid, NY). After sequential washes in TBS containing 0.1% Tween 20 and in TBS alone, ligand blots were exposed to Kodak (Rochester, NY) XAR-5 film for varying durations ranging from 1 d to 3 wk, Western blots were visualized Blots Western lighting chemiluminescence kit (PerkinElmer Life Science, Inc., Foster City, CA).

Glucose, Insulin, Total IGF-I, and Bioactive IGF-I Measurements

Mice were fasted for 16 h (1700–0900 h) followed by ip injection of glucose (2 g/kg body weight). Whole venous blood was obtained from the tail vein at the indicated time points (0, 1, 2, 5, 10, 15, 30, 60, 90, and 120 min) after the glucose injection. Blood glucose levels were measured using a Glucotrend glucometer (Johnson & Johnson, New Brunswick, NJ). To measure insulin levels and IGF levels during a glucose tolerance test, blood was collected in EDTA-containing tubes and then centrifuged. Insulin levels were measured at 0, 1, 2, 5, 10, 15, 30, 60, and 90 min using an RIA rat insulin kit (Amersham, Arlington Heights, IL). Total IGF-I levels were measured at 0, 15, 30, 60, and 90 min using an RIA rat IGF-I kit (Diagnostic Inc., Houston, TX).

Serum levels of bioactive IGF-I was measured by an in-house IGF-I kinase receptor activation assay, based on human embryonic renal cells (EBNA 293) transfected with the human IGF-I receptor gene (27). In brief, cultured cells are stimulated at 37 C with either IGF-I standards (a serial dilution ranging from 0.3 to 10 ng/ml of recombinant human IGF-I from Austral Biologicals, San Ramon, CA) or mice sera diluted 1 in 10 in Krebs Ringer buffer (KRB). After 15 min, samples are removed and the cells lysed. Then, crude cell lysates were transferred to an assay that detects the concentration of phosphorylated (*i.e.* activated) IGF-I receptors. This assay uses a monoclonal antibody against the extracellular domain of the IGF-I receptor for coating and an Europium-labeled monoclonal antiphosphotyrosine antibody (PY20) as tracer. The assay is sensitive (detection limit < 0.08 μg/liter), specific (IGF-II cross-reactivity is 12%, whereas proinsulin, insulin, and insulin analogs have a cross-reactivity $< 1\%$), and precise (mean within and in-between assay CVs were < 7 and 15%).

The bioassay was originally developed to measure IGF-I bioactivity in human serum, and therefore, we performed some studies to investigate whether the bioassay behaved similarly in mouse serum. Because the cells are not viable in undiluted serum, it is necessary to dilute serum at least 1:5 in KRB before bioassay. But it is well known that limited dilution of human serum in KRB (from 1:5 to 1:20) does not have any major effects on levels of free and bioactive IGF-I (27, 57). This observation is explained by the buffering effects of the IGFBPs, which dissociate IGF-I during dilution to maintain equilibrium (58). Therefore, we examined the effect of dilution of healthy mouse serum in KRB, which showed that bioactive IGF-I remained relatively stable when comparing pooled mouse serum diluted 1:5 and 1:10 before assay, whereas levels decreased more at a dilution of 1:20: bioactive IGF-I (μg/l): 4.30 ± 0.06 (dilution 1:5) *vs.* 3.91 ± 0.04 (dilution 1:10) *vs.* 2.29 ± 0.03 (dilution 1:20) (mean and SEM of duplicate determinations). Based on this observation, we diluted all further mouse samples 1:10 before bioassay.

The bioassay measures the ability of serum to stimulate the IGF-I receptor *in vitro*. This receptor accessible fraction of IGF-I is believed to be composed of the sum of truly free IGF-I plus IGF-I being dissociated from the IGFBPs during incubation; the latter fraction has been named "readily dissociable IGF-I" and has been suggested to be of clinical relevance

(59). Accordingly, in humans levels of bioactive IGF-I are higher than those of free IGF-I in humans (27). Therefore, levels of ultrafiltered free IGF-I *vs.* bioactive IGF-I were also compared in the same pool of healthy mouse serum, and in accordance with expectations levels of bioactive IGF-I were about 3-fold higher than those of ultrafiltered free IGF-I (data not shown), hereby supporting the concept that bioactive mouse IGF-I is also composed of the sum of free IGF-I plus readily dissociable IGF-I.

Insulin Tolerance Test

Mice were fasted for 6 h (0900–1500) followed by ip injection of recombinant human insulin (0.5 U/kg body weight; Eli Lilly, Indianapolis, IN). Whole venous blood was obtained from the tail vein at the 0, 15, 30, 60, 90, and 120 min after insulin injection. Blood glucose levels were measured using a Glucotrend glucometer (Johnson & Johnson).

Protein Purification, AKT, and MAPK Immunoblotting

Tissues from skeleton muscle were collected from six wild-type and nine triple KO mice after overnight fast. Then all tissues were lysed in modified RIPA butter [1× PBS, 1% Nonidet P-40 (Sigma, St. Louis, MO), 0.5% sodium deoxycholate, 0.1% sodium dodecyl sulfate]. A total of 10 mg/ml phenylmethylsulfonyl fluoride in isopropanol (10 μl/ml RIPA) was added at time of use. Total tissue lysates (40 μg per sample) were boiled in SDS-PAGE loading buffer, separated on 4–20% gradient gels (Invitrogen, Carlsbad, CA), and then transferred onto polyvinylidene fluoride membranes. The membrane was preblocked with blotto (5% dry milk in TBS) and incubated overnight at 4 C in antiserum against phosphor-MAPK (Cell Signaling, Danvers, MA), which visualized both phosphorated 42- and 44-kDa Erk bands. After washes in TBS and TBS plus 0.5% Tween-20, membranes were incubated in secondary antibody (horseradish peroxidase-conjugated antirabbit IgG; Promega Corp., Madison, WI) for 1 h and washed again in TBS and TBS plus 0.5% Tween 20. Blots were then visualized using Western lighting chemiluminescence kit (PerkinElmer Life Science, Inc.). Then the membranes were stripped and incubated overnight at 4 C in antiserum against MAPK to visualized nonphosphorated Erk bands using the same procedure above. Signals were scanned and band intensities were quantified by NIH software. The same procedures were performed to measure the stimulation of AKT.

Immunohistochemistry of Pancreata and Quantitation of β-Cells

Pancreata from six wild-type mice and six IGFBP-3-4-5 null mice were examined. For analysis of adult pancreata, animals were killed by overdose of sodium amytal. All pancreata were removed, cleared of fat and spleen, weighed, and fixed overnight in Bouin's solution. Then the pancreata were embedded in paraffin and consecutive sections (15 μm) were mounted on slides. After rehydration and permeabilization, one of four continuous slides was immunostained using mouse antiinsulin antibodies (Sigma), followed by detection using fluorescein antibodies (Jackson ImmunoResearch, West Grove, PA) to visualize the β-cell. To assess the morphology of pancreas, the pancreas sections were stained by H/E. For quantitation of islet area, all sections were viewed using fluorescent microscope and the staining areas were digitally photographed at a magnification of ×100. The entire sections were viewed by dissection microscope and were digitally photographed at a magnification of ×2. Analyses of islet areas and entire section areas were performed using Matlab software (Mathworks Corp., Natick, MA). Average percentage of islet areas per pancreas was measured from the total count of 48 out of 96 sections (totally over 600 islets in all cross sections) for each mouse with six wild-type mice and six IGFBP-3-4-5 mutant mice analyzed.

Statistical Analysis

Data are expressed as means ± SE. For comparison of multiple groups, an ANOVA with repeated measures followed by Student's *t* test was used. *P* value less than 0.05 shows significant difference, indicated by *, whereas *P* values less than 0.01 are indicated by**.

Acknowledgments

We are pleased to thank Bao Hoang for advice and assistance in the glucose tolerance experiments, Ming-sing Hsu for assistance with the pancreatic histology, and Mrs. Lene Ring Kristensen for helping with the kinase receptor activation assay experiments.

Received May 17, 2005. Accepted April 21, 2006.

Address all correspondence and requests for reprints to: John E. Pintar, Department of Neuroscience and Cell Biology, University of Medicine and Dentistry of New Jersey, Piscataway, New Jersey 08854. E-mail: pintar@cabm.rutgers.edu.

This work was supported by National Institutes of Health Grants NS-21970 (to J.E.P.) and DK-42748 (to P.R.), and grants from the Danish Research Council for Health and Disease (to J.F.).

REFERENCES

1. Le Roith D 2003 The insulin-like growth factor system. Exp Diabesity Res 4:205–212
2. Murphy LJ 2003 The role of the insulin-like growth factors and their binding proteins in glucose homeostasis. Exp Diabesity Res 4:213–224
3. Firth SM, Baxter RC 2002 Cellular actions of the insulin-like growth factor binding proteins. Endocr Rev 23: 824–854
4. Jones JI, Clemmons DR 1995 Insulin-like growth factors and their binding proteins: biological actions. Endocr Rev 16:3–34
5. Baxter RC 2000 Insulin-like growth factor (IGF)-binding proteins: interactions with IGFs and intrinsic bioactivities. Am J Physiol Endocrinol Metab 278:E967–E976
6. Mohan S, Baylink DJ 2002 IGF-binding proteins are multifunctional and act via IGF-dependent and -independent mechanisms. J Endocrinol 175:19–31
7. Murphy LJ 1998 Insulin-like growth factor-binding proteins: functional diversity or redundancy? J Mol Endocrinol 21:97–107
8. Clemmons DR, Busby W, Clarke JB, Parker A, Duan C, Nam TJ 1998 Modifications of insulin-like growth factor binding proteins and their role in controlling IGF actions. Endocr J 45(Suppl):S1–S8
9. Spagnoli A, Hwa V, Horton WA, Lunstrum GP, Roberts Jr CT, Chiarelli F, Torello M, Rosenfeld RG 2001 Antiproliferative effects of insulin-like growth factor-binding protein-3 in mesenchymal chondrogenic cell line RCJ3.1C5.18. Relationship to differentiation stage. J Biol Chem 276:5533–5540
10. Chen JC, Shao ZM, Sheikh MS, Hussain A, LeRoith D, Roberts Jr CT, Fontana JA 1994 Insulin-like growth factor-binding protein enhancement of insulin-like growth factor-I (IGF-I)-mediated DNA synthesis and IGF-I bind-

ing in a human breast carcinoma cell line. J Cell Physiol 158:69–78
11. Ernst M, Rodan GA 1990 Increased activity of insulin-like growth factor (IGF) in osteoblastic cells in the presence of growth hormone (GH): positive correlation with the presence of the GH-induced IGF-binding protein BP-3. Endocrinology 127:807–814
12. Angelloz-Nicoud P, Harel L, Binoux M 1996 Recombinant human insulin-like growth factor (IGF) binding protein-3 stimulates prostate carcinoma cell proliferation via an IGF-dependent mechanism. Role of serine proteases. Growth Regul 6:130–136
13. Clark RG, Mortensen D, Reifsynder D, Mohler M, Etcheverry T, Mukku V 1993 Recombinant human insulin-like growth factor binding protein-3 (rhIGFBP-3): effects on the glycemic and growth promoting activities of rhIGF-1 in the rat. Growth Regul 3:50–52
14. Hamon GA, Hunt TK, Spencer EM 1993 In vivo effects of systemic insulin-like growth factor-I alone and complexed with insulin-like growth factor binding protein-3 on corticosteroid suppressed wounds. Growth Regul 3:53–56
15. Miyakoshi N, Richman C, Kasukawa Y, Linkhart TA, Baylink DJ, Mohan S 2001 Evidence that IGF-binding protein-5 functions as a growth factor. J Clin Invest 107: 73–81
16. Stewart CE, Bates PC, Calder TA, Woodall SM, Pell JM 1993 Potentiation of insulin-like growth factor-I (IGF-I) activity by an antibody: supportive evidence for enhancement of IGF-I bioavailability in vivo by IGF binding proteins. Endocrinology 133:1462–1465
17. Zapf J 1997 Total and free IGF serum levels. Eur J Endocrinol 136:146–147
18. Martin JL, Baxter RC 1992 Insulin-like growth factor binding protein-3: biochemistry and physiology. Growth Regul 2:88–99
19. Boisclair YR, Rhoads RP, Ueki I, Wang J, Ooi GT 2001 The acid-labile subunit (ALS) of the 150 kDa IGF-binding protein complex: an important but forgotten component of the circulating IGF system. J Endocrinol 170:63–70
20. Lee CY, Rechler MM 1995 Formation of 150-kDa binary complexes of insulin-like growth factor binding protein-3 and the acid-labile subunit in vitro and in vivo. Prog Growth Factor Res 6:241–251
21. Rajkumar K, Krsek M, Dheen ST, Murphy LJ 1996 Impaired glucose homeostasis in insulin-like growth factor binding protein-1 transgenic mice. J Clin Invest 98: 1818–1825
22. Di Cola G, Cool MH, Accili D 1997 Hypoglycemic effect of insulin-like growth factor-1 in mice lacking insulin receptors. J Clin Invest 99:2538–2544
23. Schneider MR, Lahm H, Wu M, Hoeflich A, Wolf E 2000 Transgenic mouse models for studying the functions of insulin-like growth factor-binding proteins. FASEB J 14: 629–640
24. Wang J, Niu W, Witte DP, Chernausek SD, Nikiforov YE, Clemens TL, Sharifi B, Strauch AR, Fagin JA 1998 Overexpression of insulin-like growth factor-binding protein-4 (IGFBP-4) in smooth muscle cells of transgenic mice through a smooth muscle α-actin-IGFBP-4 fusion gene induces smooth muscle hypoplasia. Endocrinology 139: 2605–2614
25. Wood TL, Rogler LE, Czick ME, Schuller AG, Pintar JE 2000 Selective alterations in organ sizes in mice with a targeted disruption of the insulin-like growth factor binding protein-2 gene. Mol Endocrinol 14:1472–1482
26. Silha JV, Murphy LJ 2002 Insights from insulin-like growth factor binding protein transgenic mice. Endocrinology 143:3711–374
27. Chen JW, Ledet T, Orskov H, Jessen N, Lund S, Whittaker J, De Meyts P, Larsen MB, Christiansen JS, Frystyk J 2003 A highly sensitive and specific assay for determination of IGF-I bioactivity in human serum. Am J Physiol Endocrinol Metab 284:E1149–E1155
28. Bratanova-Tochkova TK, Cheng H, Daniel S, Gunawardana S, Liu YJ, Mulvaney-Musa J, Schermerhorn T, Straub SG, Yajima H, Sharp GW 2002 Triggering and augmentation mechanisms, granule pools, and biphasic insulin secretion. Diabetes 51(Suppl 1):S83–S90
29. Kulkarni RN 2004 The islet β-cell. Int J Biochem Cell Biol 36:365–371
30. Yamauchi T, Tobe K, Tamemoto H, Ueki K, Kaburagi Y, Yamamoto-Honda R, Takahashi Y, Yoshizawa F, Aizawa S, Akanuma Y, Sonenberg N, Yazaki Y, Kadowaki T 1996 Insulin signalling and insulin actions in the muscles and livers of insulin-resistant, insulin receptor substrate 1-deficient mice. Mol Cell Biol 16:3074–3084
31. Withers DJ, Gutierrez JS, Towery H, Burks DJ, Ren JM, Previs S, Zhang Y, Bernal D, Pons S, Shulman GI, Bonner-Weir S, White MF 1998 Disruption of IRS-2 causes type 2 diabetes in mice. Nature 391:900–904
32. Cheatham B, Kahn CR 1995 Insulin action and the insulin signaling network. Endocr Rev 16:117–142
33. LeRoith D, Werner H, Beitner-Johnson D, Roberts Jr CT 1995 Molecular and cellular aspects of the insulin-like growth factor I receptor. Endocr Rev 16:143–163
34. Baserga R, Hongo A, Rubini M, Prisco M, Valentinis B 1997 The IGF-I receptor in cell growth, transformation and apoptosis. Biochim Biophys Acta 1332:F105–F126
35. Le Roith D, Kim H, Fernandez AM, Accili D 2002 Inactivation of muscle insulin and IGF-I receptors and insulin responsiveness. Curr Opin Clin Nutr Metab Care 5:371–375
36. Wang J, Zhou J, Powell-Braxton L, Bondy C 1999 Effects of Igf1 gene deletion on postnatal growth patterns. Endocrinology 140:3391–3394
37. Domene HM, Bengolea SV, Jasper HG, Boisclair YR 2005 Acid-labile subunit deficiency: phenotypic similarities and differences between human and mouse. J Endocrinol Invest 28:43–46
38. Yakar S, Rosen CJ, Beamer WG, Ackert-Bicknell CL, Wu Y, Liu JL, Ooi GT, Setser J, Frystyk J, Boisclair YR, LeRoith D 2002 Circulating levels of IGF-1 directly regulate bone growth and density. J Clin Invest 110:771–781
39. Yakar S, Liu JL, Fernandez AM, Wu Y, Schally AV, Frystyk J, Chernausek SD, Mejia W, Le Roith D 2001 Liver-specific igf-1 gene deletion leads to muscle insulin insensitivity. Diabetes 50:1110–1118
40. Baserga R 1994 Oncogenes and the strategy of growth factors. Cell 79:927–930
41. Hu X, Jin L, Feng L 2004 Erk1/2 but not PI3K pathway is required for neurotrophin 3-induced oligodendrocyte differentiation of post-natal neural stem cells. J Neurochem 90:1339–1347
42. Freeman SM, Whartenby KA 2004 The role of the mitogen-activated protein kinase cellular signaling pathway in tumor cell survival and apoptosis. Drug News Perspect 17:237–242
43. Coleman ME, DeMayo F, Yin KC, Lee HM, Geske R, Montgomery C, Schwartz RJ 1995 Myogenic vector expression of insulin-like growth factor I stimulates muscle cell differentiation and myofiber hypertrophy in transgenic mice. J Biol Chem 270:12109–12116
44. Powell-Braxton L, Hollingshead P, Warburton C, Dowd M, Pitts-Meek S, Dalton D, Gillett N, Stewart TA 1993 IGF-I is required for normal embryonic growth in mice. Genes Dev 7:2609–2617
45. Ogus S, Ke Y, Qiu J, Wang B, Chehab FF 2003 Hyperleptinemia precipitates diet-induced obesity in transgenic mice overexpressing leptin. Endocrinology 144: 2865–2869
46. Porksen N, Hussain MA, Bianda TL, Nyholm B, Christiansen JS, Butler PC, Veldhuis JD, Froesch ER, Schmitz O 1997 IGF-I inhibits burst mass of pulsatile insulin se-

cretion at supraphysiological and low IGF-I infusion rates. Am J Physiol 272:E352–E358
47. Bruning JC, Michael MD, Winnay JN, Hayashi T, Horsch D, Accili D, Goodyear LJ, Kahn CR 1998 A muscle-specific insulin receptor knockout exhibits features of the metabolic syndrome of NIDDM without altering glucose tolerance. Mol Cell 2:559–569
48. Leahy JL, Vandekerkhove KM 1990 Insulin-like growth factor-I at physiological concentrations is a potent inhibitor of insulin secretion. Endocrinology 126:1593–1598
49. Funaki M, Randhawa P, Janmey PA 2004 Separation of insulin signaling into distinct GLUT4 translocation and activation steps. Mol Cell Biol 24:7567–7577
50. Gual P, Le Marchand-Brustel Y, Tanti J 2003 Positive and negative regulation of glucose uptake by hyperosmotic stress. Diabetes Metab 29:566–575
51. Hill DJ, Petrik J, Arany E, McDonald TJ, Delovitch TL 1999 Insulin-like growth factors prevent cytokine-mediated cell death in isolated islets of Langerhans from pre-diabetic non-obese diabetic mice. J Endocrinol 161:153–165
52. Giannoukakis N, Mi Z, Rudert WA, Gambotto A, Trucco M, Robbins P 2000 Prevention of β cell dysfunction and apoptosis activation in human islets by adenoviral gene transfer of the insulin-like growth factor I. Gene Ther 7:2015–2022
53. Rossetti L, Frontoni S, Dimarchi R, DeFronzo RA, Giaccari 1991 Metabolic effects of IGF-I in diabetic rats. Diabetes 40:444–448
54. Simpson HL, Umpleby AM, Russell-Jones DL 1998 Insulin-like growth factor-I and diabetes. A review. Growth Horm IGF Res 8:83–95
55. Guler HP, Zapf J, Froesch ER 1987 Short-term metabolic effects of recombinant human insulin-like growth factor I in healthy adults. N Engl J Med 317:137–140
56. Lewitt MS, Denyer GS, Cooney GJ, Baxter RC 1991 Insulin-like growth factor-binding protein-1 modulates blood glucose levels. Endocrinology 129:2254–2256
57. Frystyk J, Skjaerbaek C, Dinesen B, Orskov H 1994 Free insulin-like growth factors (IGF-I and IGF-II) in human serum. FEBS Lett 348:185–191
58. Ekins R 1990 Measurement of free hormones in blood. Endocr Rev 11:5–46
59. Juul A, Skakkebaek NE 1997 Prediction of the outcome of growth hormone provocative testing in short children by measurement of serum levels of insulin-like growth factor I and insulin-like growth factor binding protein 3. J Pediatr 130:197–204

Molecular Endocrinology **is published monthly by The Endocrine Society (http://www.endo-society.org), the foremost professional society serving the endocrine community.**